6th IFAC Symposium Advances in Automotive Control
Munich, Germany, July 12-14, 2010

Autonomous Cornering at the Limits: Maximizing a "g-g" Diagram by Using Feedforward Trail-Braking and Throttle-on-Exit

Krisada Kritayakirana * **J. Christian Gerdes** **

* *Dynamic Design Laboratory, Department of Mechanical Engineering, Stanford University, Stanford, CA 94305 USA, e-mail: krisadak@stanford.edu*
** *e-mail: gerdes@stanford.edu*

Abstract:
This paper explains the design of a feedforward longitudinal controller that will drive an autonomous vehicle through a corner at the limits of tire adhesion. The feedforward longitudinal algorithm applies appropriate amounts of braking force and throttle during cornering to mimic a racecar driver trail-braking into a corner and applying the throttle during corner exit. A "g-g" diagram combined with a clothoid map is used to estimate the feedforward longitudinal command. By introducing this feedforward algorithm into the controller, significant improvements in lap time and cornering exit speed were observed. Analyzing the controller performance during cornering also provides an insight to the future development of the feedback longitudinal controller. The knowledge gained from designing an algorithm that controls a vehicle at the limits can be applied to future driver assistance systems to make cars safer, yet still fun to drive.

Keywords: Vehicle Dynamics, Autonomous Driving, Vehicle Dynamics Control, "g-g" diagram, Clothoid, Trail-Braking, Throttle-on-Exit.

1. INTRODUCTION

This research aims to develop a controller that can drive an autonomous vehicle to its maximum potential. The controller is designed to imitate racecar drivers' abilities to control a vehicle at the limits of handling. By understanding how to control a vehicle at its limits, this knowledge can be applied to design better driver assistance systems. For instance, future systems could constantly and seamlessly provide combinations of steering, throttle, and brake to ensure that the driver remains in control of the vehicle at all times.

Racecar drivers have three key characteristics that help them to operate a vehicle at the limits without losing control. First, they can sense the available friction between the tires and the road (gauging how much control authority they have). Secondly, they have the ability to utilize every actuator (steering, throttle, shifting, and brake) to control the motion of a vehicle (van Zanten et al. (1996)). Finally, they know how to choose an optimum path (racing line). The work in this paper is focused on the vehicle control part, and assumes that the controller has a priori knowledge of friction and the desired path. Various techniques, including friction estimation based on steering torque (Hsu and Gerdes (2008)), can be used in the future to imitate racecar drivers' ability to sense the friction.

In previous work (Kritayakirana and Gerdes (2009)), a controller was designed to drive an autonomous vehicle through a corner at the limits of handling with minimal tracking error. However, as the approach was based on a steady state cornering assumption, the vehicle entered and exited the corner at a constant speed and reached the limits of cornering only at the mid corner section. Thus, to fully utilize the limits of friction during corner entry and exit, this paper extends the algorithm to include trail-braking and throttle-on-exit techniques (Lopez (2001); Velenis et al. (2007)) in the feedforward longitudinal algorithm.

This paper starts with explaining how friction forces from the tires bound the acceleration plot on a "g-g" diagram. To maximize speed and reduce time, the feedforward longitudinal command is designed to make the vehicle's acceleration trace this limit by using trail-braking and throttle-on-exit techniques. Because the vehicle's acceleration consists of lateral and longitudinal components during cornering, knowledge of the lateral acceleration is required to calculate the feedforward longitudinal command. As the lateral acceleration of a vehicle depends on the track curvature, a clothoid map with linearly varying curvature is introduced to facilitate the computation of the lateral acceleration. Once the knowledge of the lateral motion is established, the feedforward longitudinal command can be found from the limit of the "g-g" diagram. Coupled with a steering controller, longitudinal feedback and feedforward controllers are then implemented on a test vehicle. A plot of the vehicle's acceleration tracing along the limit on a

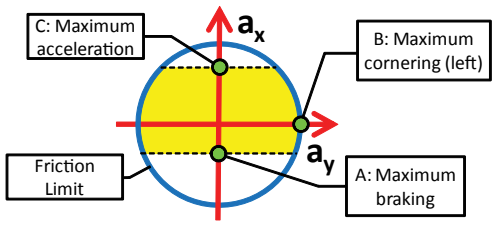

Fig. 1. Introduction to a "g-g" diagram

"g-g" diagram is demonstrated in the results section. The effectiveness of the feedforward trail-braking and throttle-on-exit along with an explanation of the control actuation sequence are discussed before ending with future development of the feedback longitudinal controller.

2. "g-g" DIAGRAM

Racecar drivers try to maximize the friction forces from the tires while going through a corner at speed. To mimic this behavior, the feedforward longitudinal controller should ensure that the vehicle fully utilizes the friction forces during cornering. However, estimating the available friction forces from the tires is complicated because each tire can generate a different amount of friction force. Many factors such as normal loads and suspension geometries influence the maximum force that an individual tire can provide. To reduce the complexity, the concept of a "g-g" diagram, which lumps all four tires together, is used (Rice (1973); Milliken and Milliken (1995)).

Driver performance can be evaluated on a "g-g" diagram by observing how close the driver gets to the friction limit while driving, see Fig. 1. This friction limit in a "g-g" diagram is found by assuming that all four tires reach their limits at once. The total friction force F will equal to the normal force (or the vehicle weight, when ignoring the aerodynamic force) times the friction coefficient μ. By using Newton's second law, the maximum acceleration that the vehicle could generate is equal to μg, where g is the acceleration due to gravity. This acceleration limit forms the circle in Fig. 1. Consequently, the goal of the feedforward longitudinal controller is to make the acceleration of the vehicle trace along this circle. Note that the vehicle could have limited braking and accelerating capabilities (dashed lines in Fig. 1), which bound the acceleration that the vehicle can generate and restrict the motion of the vehicle to a subset of the friction circle (shaded region).

To trace along the circle, the feedforward longitudinal controller has to apply the correct amount of longitudinal acceleration. For instance, when combining the lateral acceleration from cornering with longitudinal acceleration, the combined acceleration must be at the limit. Thus, to accurately predict the amount of cornering along the track, the knowledge of the path is required. As a consequence, a track that has curvature that is smoothly varying and easy to identify has to be created.

3. CLOTHOID MAP

Tracing along the circle in Fig. 1 requires the knowledge of lateral acceleration a_y to estimate the longitudinal acceleration a_x. To reduce the complexity of this calculation, a

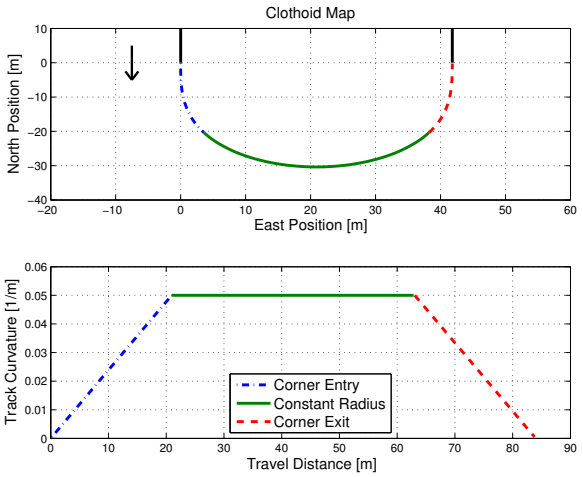

Fig. 2. Clothoid map: showing shape and curvature

map with a linear relationship between the track curvature and the path is desired. Thus, a clothoid map (also known as an Euler Spiral, and a common practice in highway road design, AASHTO (2004)) is chosen for designing the feedforward longitudinal controller. It is important to note that while such a map has nice mathematical properties, it may or may not represent the actual racing line that a racecar driver uses.

A clothoid map is generated by using a Fresnel Integral (Jeffrey and Dai (2008)). The position East x and position North y can be found from:

$$\begin{aligned} x &= C(\acute{s}) = \frac{1}{c}\int_0^{\acute{s}} \cos(q^2)\,dq \\ y &= S(\acute{s}) = \frac{1}{c}\int_0^{\acute{s}} \sin(q^2)\,dq \end{aligned} \tag{1}$$

where $\acute{s} = cs$ and $c = \frac{1}{\sqrt{2sR}}$. s is the distance measured along the clothoid segment. R is the radius of the clothoid curvature along s. The value c controls the rate that the curvature changes along the segment, i.e. the slope of the curvature in Fig. 2.

To show that the clothoid curvature has a linear relationship with the traveled distance s, the curvature k of a track can be found from:

$$k = \frac{1}{R} = \frac{\dot{x}\ddot{y} - \dot{y}\ddot{x}}{(\dot{x}^2 + \dot{y}^2)^{\frac{3}{2}}} \tag{2}$$

where $\dot{x} = \frac{dx}{ds}$,$\dot{y} = \frac{dy}{ds}$, $\ddot{x} = \frac{d^2x}{ds^2}$, and $\ddot{y} = \frac{d^2y}{ds^2}$. By substituting x and y from equation (1) into equation (2), the clothoid curvature is found to be:

$$k = \frac{1}{R} = 2c^2 s \tag{3}$$

This linear relationship between the curvature and traveled distance will be used in section 4.

In addition, as the feedforward steering is calculated from the track curvature, the smoothness of the curvature transition along the clothoid path will produce smooth feed-

forward steering. In previous work, which used a polynomial based map (Rossetter et al. (2004)) to calculate the feedforward steering, there were abrupt changes in the feedforward steering input. These sudden changes were caused by the unevenness of the second derivatives values in equation (2). This undesired steering motion caused the vehicle to oscillate along the path, creating a yaw motion and unnecessary front tire slip, which became a critical issue during cornering at the limits. When using a clothoid map, the transition of the curvature along the path is smooth and results in smooth feedforward steering.

4. LONGITUDINAL FEEDFORWARD CONTROLLER

The goal of the longitudinal feedforward algorithm is to design throttle and brake inputs that mimic a racecar driver trail-braking into a corner and applying the throttle on corner exit. That is, the vehicle's acceleration plot should trace the circle in Fig. 1.

The example curve in Fig. 2 is divided into three sections: clothoid entry (corner entry), constant radius (mid corner), and clothoid exit (corner exit). As the feedforward calculation for the clothoid exit section is more intuitive to understand, this section is explained first.

Clothoid Exit: During corner exit, the driver transitions from full cornering (point B in Fig. 1) to full accelerating (point C in Fig. 1). The racecar driver progressively applies throttle while controlling the steering wheel to balance between longitudinal acceleration a_x and lateral acceleration a_y. Thus, the goal of the feedforward longitudinal control is to calculate the correct amount of a_x at each point along the segment s, so that when combined with the a_y generated from vehicle cornering, the vehicle's acceleration will trace counterclockwise along the first quadrant of the circle.

From Section 2, the maximum acceleration that the vehicle can achieve is μg regardless of the direction. Thus, the relation between a_x and a_y at the limits is:

$$(\mu g)^2 = a_x^2 + a_y^2 \tag{4}$$

To estimate the feedforward longitudinal acceleration along the segment s, the calculation starts by using a steady state cornering assumption to approximate a_y:

$$a_y \approx \frac{U_x(s)^2}{R} = U_x(s)^2 k \tag{5}$$

where $U_x(s)$ is the the estimated longitudinal speed along the path s. If $U_x(s)$ is known at a given point, then a_y can be estimated. To trace along the circle, the combination of a_x and a_y has to follow equation (4). Thus, by knowing a_y, a_x can be found.

To find $U_x(s)$ at any given point s, the calculation starts from substituting a_y from equation (5) and k from equation (3) into equation (4), and rearranging to obtain:

$$a_x = \sqrt{(\mu g)^2 - (2c^2 s U_x(s)^2)^2} \tag{6}$$

From the differential equation of a_x:

$$a_x = \frac{dU_x(s)}{dt} = \frac{dU_x(s)}{ds}\frac{ds}{dt} = \frac{dU_x(s)}{ds}U_x(s)$$

where t is time. Substituting this definition of a_x into equation (6) obtains:

$$\frac{dU_x(s)}{ds} = \frac{1}{U_x(s)}\sqrt{(\mu g)^2 - (2c^2 s U_x(s)^2)^2} \tag{7}$$

In order to solve equation (7) real-time on an experimental vehicle, $U_x(s)$ can be approximated by using a backward integration as follows:

$$U_x(s_{n+1}) \approx U_x(s_n) + \frac{\Delta s}{U_x(s_n)}\sqrt{(\mu g)^2 - (2c^2 s_n U_x(s_n)^2)^2} \tag{8}$$
$$\Delta s = s_{n+1} - s_n$$

for $n = 0, 1, 2, ..., L^{cloth}/\Delta s$, where $s_n = n\Delta s$ is the distance along the segment. L^{cloth} is the length of the clothoid section. In this paper, $\Delta s = 0.1m$.

At the beginning of the clothoid exit, $s_0 = 0$, the vehicle is at point B in Fig. 1, where $a_x = 0$ while $a_y = \mu g$. The speed at this point, $U_x(0)$, can be found from approximating a_y by using equation (5). As a consequence, $U_x(0) = \sqrt{\mu R(0) g}$, where $R(0)$ is the curvature of the constant radius in the mid corner section.

$U_x(s)$ along the clothoid exit is found from equation (8). Then, the component of the feedforward longitudinal acceleration a_x along s can be found from equation (6).

Clothoid Entry: During corner entry, the driver transitions from full braking (point A in Fig. 1) to full cornering (point B). A trail-braking technique is used to trace along the circle by modulating the correct amount of brake and steering.

Similar to the clothoid exit, calculating the feedforward longitudinal acceleration a_x starts from estimating U_x along the clothoid section by using equation (8). However, equation (8) has to be integrated backward from the end of the clothoid where $s = L^{cloth}$, to the beginning of the clothoid where $s = 0$. The initial condition at $s = L^{cloth}$ is the same initial condition as for the clothoid exit calculation.

Furthermore, because the research vehicle available for testing uses regenerative braking, which cannot generate any braking forces lower than $-1.8m/s^2$, equation (8) must be modified:

$$U_x(s_{n+1}) \approx U_x(s_n) + \frac{\Delta s}{U_x(s_n)}|a_x^{regen}|$$

whenever the calculated feedforward a_x is less than the regenerative braking limit a_x^{regen}. Note that s in this case is progressing backward along the path.

One of the key parameters in this section is the calculated corner entry speed that came from equation (8). Although the longitudinal feedforward only focuses on a_x, this corner entry speed is important because it influences the subsequent a_y, from equation (5), and effectively dictates how a vehicle will corner from equation (4).

Constant Radius: At mid corner, the vehicle is operating at maximum cornering (point B in Fig. 1). In theory, the longitudinal feedforward should not apply any a_x to

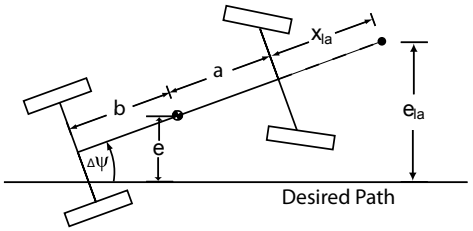

Fig. 3. Definition of lateral error (e), heading error ($\Delta\psi$), and lookahead error (e_{la})

maximize a_y. However, without any throttle, the vehicle tends to slow down because of the rolling resistance and because the drag from the lateral forces at the front wheels has a longitudinal component. Thus, a simple proportional speed feedback is applied to ensure that the vehicle tracks the feedforward speed of $\sqrt{\mu R(0)g}$.

5. LONGITUDINAL FEEDBACK CONTROLLER AND STEERING CONTROLLER

5.1 Longitudinal Feedback Algorithm

The longitudinal feedback imitates racecar drivers feathering their throttle and brake during cornering to minimize tracking error and time.

The longitudinal feedback uses proportional feedback based on the absolute value of the heading error $\Delta\psi$ (see Fig. 3). Pervious work showed that $\Delta\psi$ increased when the vehicle was going too fast because of the limit-understeer characteristic of the vehicle. Thus, using the absolute value of $\Delta\psi$ will ensure that the feedback will command braking force whenever $\Delta\psi$ deviates from zero.

$$F_x^{feedback} \propto -|\Delta\psi| \tag{9}$$

5.2 Steering Controller

The steering controller consists of feedforward and feedback steering. The feedforward steering is similar to a driver planning the amount of turning before going into a turn while feedback steering imitates a driver adjusting the steering to mitigate tracking errors.

Feedforward Steering The feedforward steering equation is derived from a linear bicycle model (Kritayakirana and Gerdes (2009)). After substituting the curvature $1/R$ from equation (3), the feedforward steering becomes:

$$\delta_{feedforward} = (L + \frac{KU_x^2}{g})\frac{1}{R} = (L + \frac{KU_x^2}{g})2c^2 s \tag{10}$$

where K is the understeer gradient and L is the vehicle length. With a clothoid map, the feedforward steering is proportional to the progress along the segment s and does not have any abrupt changes caused by the curvature.

Feedback Steering The feedback steering mitigates any errors caused by modeling discrepancies or disturbances in the system. It is based on a potential field lanekeeping system (Rossetter et al. (2004); Hindiyeh et al. (2008)), which is proportional to the lookahead error e_{la}, shown in Fig. 3.

Fig. 4. Stanford P1 by-wire research vehicle

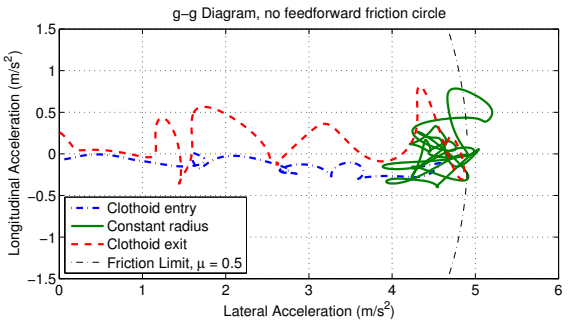

Fig. 5. "g-g" diagram: without trail-braking and throttle-on-exit

Table 1. Demonstrating feedforward longitudinal controller performance

Trail-braking & throttle-on-exit	Time Duration (s) Entry	Mid	Exit	Lap	Exit speed (m/s)
No	1.674	3.316	1.720	18.588	7.50
Yes	1.434	3.448	1.516	16.674	10.17

$$\delta_{feedback} = -\frac{2K_p}{C_f} e_{la} \tag{11}$$

where K_p is the lanekeeping potential field gain and C_f is the front axle cornering stiffness.

6. EXPERIMENTAL SETUP

The Stanford P1 by-wire research vehicle (Laws et al. (2005)), shown in Fig. 4, was used for testing on a gravel surface. The vehicle is equipped with a Differential Global Positioning System (DGPS) and inertial sensors (INS), from which vehicle position and other states can be obtained. The algorithm, described in Rossetter et al. (2004), utilizes the information from DGPS and INS to find the vehicle's path tracking errors.

To convert from the feedforward longitudinal acceleration a_x in Section 4 to a motor drive torque command, a lookup table is used.

7. EXPERIMENTAL RESULTS

In previous work, the feedforward longitudinal command was set to maintain a constant speed so that the car could corner at the maximum lateral acceleration. The "g-g" diagram of this approach is shown in Fig. 5. As expected, the vehicle operated at its limit during the mid corner section where the curvature was constant. However, during the transient maneuvers, such as corner entry and corner exit, the results demonstrated that the vehicle did not fully utilize the available friction. Lack of feedforward trail-

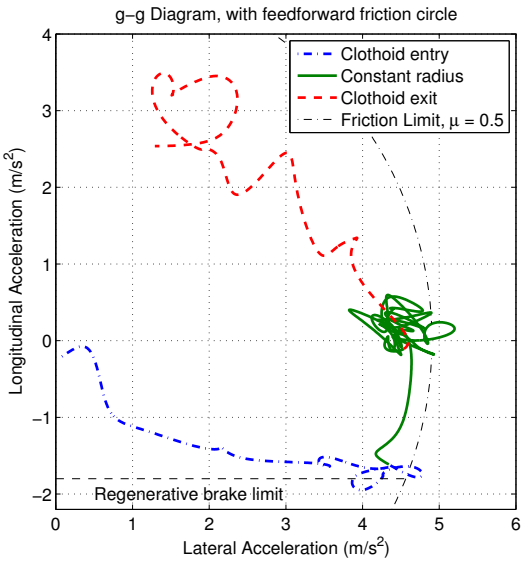

Fig. 6. "g-g" diagram: with trail-braking and throttle-on-exit

braking during corner entry and acceleration out from the exit prevented the vehicle from maximizing its potential.

After adding the feedforward trail-braking and throttle-on-exit described in this paper, the "g-g" diagram in Fig. 6 shows a better utilization of the friction limits. The vehicle reaches the regenerative braking limit during corner entry and uses the friction limit at the mid corner section, similar to the ideal trajectory shown in Fig. 1. During the corner exit, the vehicle accelerates out from the corner with some deviation in a_x from the friction limit. This deviation could be caused by the motors only driving the two rear wheels (not all four wheels), or because the motors are incapable of accelerating the vehicle at μg. In addition, note that the lookup table that mapped the desired a_x to the motor commands could have some error, which caused the actual a_x to deviate from the desired a_x.

A significant time improvement is observed in table 1 when feedforward trail-braking and throttle-on-exit are added. When analyzing each section of the corner, considerable time improvement from maximizing the acceleration can be observed during the entry and exit sections. Note that when using feedforward trail-braking and throttle-on-exit, the section time in the mid corner is slower by a small amount, which could be caused by friction variation from the gravel surface. Another critical aspect that affects the lap time is the corner exit speed. When using throttle-on-exit, a much faster exit speed was achieved. This significantly reduces the time of the following straight section.

To understand how the controller operates, the results from each corner section are analyzed.

Clothoid Entry: As shown in Fig. 7, during $27.6 - 29s$, the vehicle is trail-braking into a corner while increasing the steering angle. The speed of the vehicle U_x reduces while the yaw rate, front slip angle, and rear slip angle increase simultaneously. Notice that the $-0.9\,Volt$ of the longitudinal command corresponds to the regenerative braking limit of $-1.8m/s^2$.

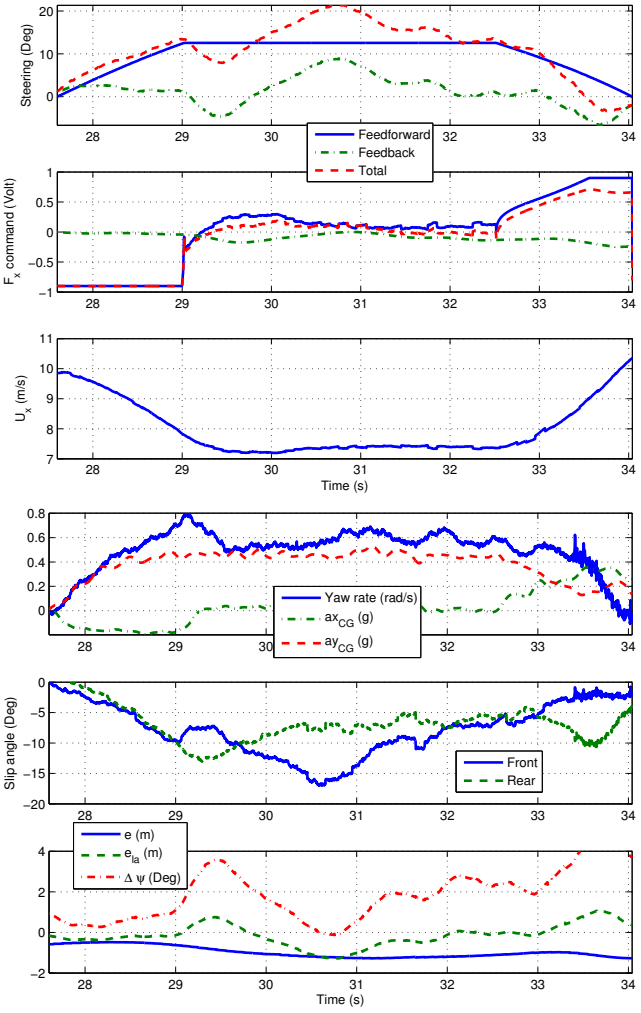

Fig. 7. Plots of input commands and vehicle states

Furthermore, notice that in Fig. 6, the vehicle did not enter the corner with full braking (point A in Fig. 1). Although the feedforward longitudinal controller commanded large braking at the beginning of the corner entry, there was a delay in the regenerative system. Full braking was not achieved until after $28s$. Hence, the vehicle was cornering at a speed higher than the desired speed $U_x(s)$. Moreover, even though the feedforward longitudinal controller was supposed to command zero braking at the end of corner entry (point B in Fig. 1), there was a delay between the longitudinal command and the actual torque at the road wheels. Consequently, the trace of the clothoid entry in Fig. 6 did not end with zero longitudinal accerelation.

Constant Radius: Between $29 - 32.5s$, the feedforward longitudinal controller tried to track a constant speed of $\sqrt{\mu R(0)g}$. As the vehicle entered the mid section with excessive speed, the longitudinal controller commanded braking while cornering and as a result, the plot traces the circle to the maximum a_y point. In order to trace the circle, all four tires have to operate at their friction limits. This means that some of the tires are sliding, as indicated by the axle slip angles plot in Fig. 7. After the vehicle tracked the desired speed and a_x became zero, the maneuver was concentrated at the maximum cornering a_y, as expected.

At around $29s$, the vehicle starts to oversteer because the regenerative braking was only applied to the rear wheels. The lanekeeping steering reacted by counter steering, which promptly reduced the front slip angle and the yaw rate, while the rear slip angle slowly decreased through the vehicle dynamics. Between $29.7 - 30.7s$, the front slip angle grows, demonstrating that the vehicle starts to understeer. Note that in this case, the heading error ($\Delta\psi$) actually reduces; thus, the longitudinal feedback based on $\Delta\psi$ did not try to slow the vehicle down. As the front tires saturated, lanekeeping steering could not generate any additional force at the front wheels to pull the vehicle back to the path and to reduce the lateral error e.

Clothoid Exit: During $32.5 - 34s$, the feedforward longitudinal controller applied throttle during corner exit. The rear slip angle increases because a large amount of longitudinal force was commanded to the rear wheels. The vehicle starts to oversteer and causes $\Delta\psi$ to increase. Longitudinal feedback based on $\Delta\psi$ detects this and commands the vehicle to slow down. It is also interesting to point out that the vehicle exited the corner while still generating lateral acceleration. Although this may lead to some tracking error, it could be beneficial not to let off the throttle to achieve faster time.

Although there is a noticeable lateral error (e) in Fig. 7, it must be noted that the objective of the lanekeeping steering feedback is to minimize the lookahead error (e_{la}), see equation (11). Better tracking performance in e can be achieved by incorporating tire saturation into the feedforward steering command and by minimizing tires sliding through a better longitudinal feedback controller.

The results demonstrate that the feedforward longitudinal controller tries to utilize the friction force from the tires. Because the feedforward calculation is based on the assumption that all four tires are operating at their friction limits, in practice, this occasionally results in some of the tires sliding. Thus, the controller relies on a good longitudinal feedback to ensure that there is no excessive slip on each tire. Although using a simple heading error ($\Delta\psi$) as a state for longitudinal feedback works well when there is no significant change in the vehicle speed, the result in the mid corner section indicates that $\Delta\psi$ could not detect that the front tires were sliding. Thus, future work will involve more complex longitudinal feedback based on a slip circle. With this new approach, the longitudinal feedback will always try to push the tires to the limits without exceeding them. Operating the front tires within their limits will prevent the front tires from sliding. Consequently, this will ensure that the lanekeeping system has control authority via the front tires, which should result in better tracking performance. In addition, the authors will start exploring the tradeoff between minimizing the tracking error and time.

8. CONCLUSION

By incorporating feedforward trail-braking and throttle-on-exit into the longitudinal controller, the results showed a better lap time as well as a faster corner exit speed. Plotting the vehicle's acceleration on a "*g-g*" diagram demonstrated that the acceleration traced the acceleration limit circle. Further refinement will involve testing the same algorithm on a different vehicle to investigate the effects of actuator limitations. Experimental results also indicated a limitation of using the heading error as a state for the longitudinal feedback. Thus, future work will involve designing a longitudinal feedback controller based on a slip circle that will work efficiently with the feedforward trail-braking and throttle-on-exit.

ACKNOWLEDGEMENTS

This research is supported by the Volkswagen Automotive Innovation Lab (VAIL) and Electronics Research Laboratory of Volkswagen of America (ERL), with additional support from a Fulbright Science and Technology Fellowship. The authors would also like to thank Dynamic Design Lab colleagues for their valuable comments on this paper and the City of Mountain View, CA for their assistance with testing.

REFERENCES

AASHTO (2004). *AASHTO Green Book: A Policy on Geometric Design of Highways and Streets*. American Association of State Highway and Transportation Officials, 5th edition.

Hindiyeh, R.Y., Talvala, K.L.R., and Gerdes, J.C. (2008). Lanekeeping at the handling limits. International Symposium on Advanced Vehicle Control (AVEC), Kobe, Japan.

Hsu, Y.H.J. and Gerdes, J.C. (2008). The predictive nature of pneumatic trail: Tire slip angle and peak force estimation using steering torque. International Symposium on Advanced Vehicle Control (AVEC), Kobe, Japan.

Jeffrey, A. and Dai, H.H. (2008). *Handbook of Mathematical Formulas and Integrals*. Academic Press, 4th edition.

Kritayakirana, K. and Gerdes, J.C. (2009). Controlling an autonomous racing vehicle: Using feedforward and feedback to control steering and speed. ASME 2009 Dynamic Systems and Control Conference.

Laws, S., Gadda, C., Kohn, S., Yih, P., Gerdes, J.C., and Milroy, J.C. (2005). Steer-by-wire suspension and steering design for controllability and observability. In *IFAC World Congress, Prague, Czech Republic*.

Lopez, C. (2001). *Going Faster! Mastering the Art of Race Driving*. Bentley Publishers, 73-90.

Milliken, W.F. and Milliken, D.L. (1995). *Race Car Vehicle Dynamics*. SAE International No. R-146, 345-359.

Rice, R.S. (1973). Measuring car-driver interaction with the g-g diagram. *Society of Automotive Engineers, Warrendale, PA*, (SAE Paper No. 730018).

Rossetter, E.J., Switkes, J.P., and Gerdes, J.C. (2004). Experimental Validation of the Potential Field Lanekeeping System. *International Journal of Automotive Technology*, 5(2), 95–108.

van Zanten, A.T., Erhardt, R., Pfaff, G., Kost, F., Hartmann, U., and Ehret, T. (1996). Control aspects of the bosch-vdc. In *International Symposium on Advanced Vehicle Control (AVEC), Aachen University of Technology, Germany*, 573–608.

Velenis, E., Tsiotras, P., and Lu, J. (2007). Modeling aggressive maneuvers on loose surfaces: The cases of trail-braking and pendulum-turn. In *European Control Conference, Kos, Greece, July 2-5, 2007*. European Control Conference.